

Article

Properties of Tool Steels and Their Importance When Used in a Coated System

Bojan Podgornik *, Marko Sedlaček, Borut Žužek and Agnieszka Guštin

Institute of Metals and Technology, SI-1000 Ljubljana, Slovenia; marko.sedlacek@imt.si (M.S.); borut.zuzek@imt.si (B.Ž.); agnieszka.gustin@imt.si (A.G.)

* Correspondence: bojan.podgornik@imt.si; Tel.: +386-1-4701-930

Received: 29 January 2020; Accepted: 10 March 2020; Published: 12 March 2020



Abstract: The introduction of new light-weight high-strength materials, which are difficult to form, increases demands on tool properties, including load-carrying capacity and wear resistance. Tool properties can be improved by the deposition of hard coatings but proper combination and optimization of the substrate properties are required to prepare the tool for coating application. The aim of this paper is to elaborate on tool steel substrate properties correlations, including hardness, fracture toughness, strength and surface quality and how these substrate properties influence on the coating performance. Results show that hardness of the steel substrate is the most influential parameter for abrasive wear resistance and load-carrying capacity, which is true for different types of hard coatings. However, high hardness should also be accompanied by sufficient fracture toughness, especially when it comes to very hard and brittle coatings, thus providing a combination of high load-carrying capacity, good fatigue properties and superior resistance against impact wear. Duplex treatment and formation of a compound layer during nitriding can be used as an additional support interlayer, but its brittleness may result in accelerated coating cracking and spallation if not supported by sufficient core hardness. In terms of galling resistance, even for coated surfaces substrate roughness and topography have major influence when it comes to hard ceramic coatings, with reduced substrate roughness and coating post-polishing providing up to two times better galling resistance.

Keywords: tool steel substrate; coatings; hardness; fracture toughness; load-carrying capacity; wear

1. Introduction

In forming applications of modern metallic materials, including die casting, stamping, forging and rolling, tool lifetime is limited due to very demanding working conditions. These include mechanical, thermal and impact loading [1,2]. Under such complex working conditions, comprising high contact stresses as well as abrasive and adhesive wear [3–5], tool surfaces are attacked by different wear and fatigue mechanisms [6–8]. By the current demands on reducing mass and size of components, lowering fuel consumption and CO₂ emission, increasing recycling and improving overall strength and safety [9,10]—especially when talking about transportation and energy sector—tools are exposed to new and more severe requirements and demands. This is related to design of the tool, selection of material and heat treatment [11], and surface engineering, where substrate preparation is essential [12].

Increased demands mean strengthened requirements in terms of the tool material properties, including temperature resistance, strength, shock and fatigue resistance, impact and sliding wear resistance, etc. Ductility and fracture toughness are among the main tool properties essential for the majority of forming applications and the influencing of tool resistance [13,14]. Properties of the tool core material, i.e., tool steel, depend on its chemical composition and production process, but primarily on the heat treatment parameters. Heat treatment defines final microstructure and corresponding

properties. In general, steel properties, mainly focused on strength and hardness are provided by a well-defined heat treatment process, consisting of an austenitization treatment with a subsequent quenching and a multiple tempering [13,15]. Typically, a trade-off between toughness and hardness is required [16]. On the other hand, through optimized heat treatment procedures, involving vacuum hardening, selection of tempering and austenitizing temperature, and inclusion of deep cryogenic treatment [17], fine-grained microstructure with homogeneous carbides distribution can be obtained [15]. Thus, improved toughness and fatigue resistance is obtained while maintaining high strength and hardness [18].

The typical property used for the planning of heat treatment for tool steels is hardness. High hardness is related to abrasive wear resistance and resistance to plastic deformation. However, beside hardness there are also other material properties, which are based on the application and surface engineering techniques, which become more important as we use tools that are more complex. These include fracture toughness, compressive and bending strength, creep and wear resistance, machinability, etc. [2]. Different material properties are defined and determined by different standards and test methods. However, each standard and test method uses specific test specimens with different geometries. Different geometries relate to different heat treatment conditions, and thus in microstructure deviation [19] and problematic properties correlation. On the other hand, circumferentially notched and fatigue-pre-cracked tensile bar (CNPTB) specimens used for measuring fracture toughness of more brittle materials, i.e., tool steels have been found as the best alternative, allowing determination and correlation of many different properties [20]. The advantage of the CNPTB specimen is in its radial symmetry and uniform microstructure through the whole volume.

Introduction of light-weight high-strength materials, being very difficult to form also sets more demanding properties requirements on tool properties, especially its surface and wear resistance [21]. One way of improving wear properties of the tool is application of different heat and diffusion treatments, i.e., plasma nitriding, thus modifying surface microstructure and properties [22,23]. Another way, proven in cutting tool applications is deposition of wear resistant coatings [24]. However, limited load-carrying capacity, adhesion and topographical characteristics of the substrate restrict successful application of hard wear-resistant coatings on forming tools. Thus, proper combination and optimization of the substrate properties are needed in order to prepare tools for coating deposition and provide improve performance of the tool [23–27].

The aim of this research work, carried out by using CNPTB test specimen configuration was to determine correlations between different tool steel properties, including fracture toughness, hardness, compressive and bending strength, wear resistance and surface quality and how these substrate properties influence on the coating performance.

2. Materials and Methods

2.1. Materials

Two tool steels being the most common in forming and tooling industry have been included in this investigation. First one, aimed at studying the effect of heat treatment parameters as well as additional plasma nitriding on the tool steel substrate properties, their correlation and influence on the load-carrying capacity and sliding wear resistance was conventional AISI H11 type hot-work tool steel (H11), produced through casting, electro slag re-melting, forging and annealing. The second one was high fatigue strength P/M cold work tool steel (PM-CW), aimed at determining the influence of hardness and fracture toughness as well as surface preparation on the load-carrying capacity as well as impact and galling wear resistance when coated with different type of hard coatings. Chemical composition of the investigated tool steels is given in Table 1.

Table 1. Chemical composition of the investigated tool steels (wt %).

No.	Tool Steel	% C	% Si	% Mn	% Cr	% Mo	% V	% W	% Co	% Fe
1	H11	0.37	<1.0	0.27	5.16	1.28	0.41	–	–	balance
2	PM-CW	0.85	0.54	0.39	4.36	2.79	2.11	2.54	4.52	balance

2.2. Heat Treatment and Coatings

Heat treatment of hot work tool steel (H11) included vacuum heat treatment performed in Ipsen VTC 324-R horizontal vacuum furnace (Ipsen, Kleve, Germany). The specimens machined from soft annealed material were preheated to 850 °C and then progressively heated at 10 °C/min to the austenitizing temperature of 990–1000 and 1030 °C, respectively, soaked for 20 min and quenched in N₂ gas flow at a cooling speed of 3 °C/s. After quenching specimens were double tempered for 2 h. First tempering was always performed at 540 °C, immediately followed by second tempering at six different temperatures, varied from 550 to 630 °C.

Specimens planned to investigate the effect of heat treatment parameters on the load-carrying capacity and sliding wear were further plasma nitrided in a Metaplas Ionon HZIW 600/1000 reactor (Metaplas Ionon, Bergisch Gladbach, Germany), surface polished and coated. Plasma nitriding was performed at 540 °C for 20 h using different gas mixtures. One group of test specimens was treated in 25% N₂:75% H₂ gas mixture, resulting in diffusion zone of about 260 µm and approx. 5 µm thick top compound layer. Another group was treated in 5% N₂:95% H₂ gas mixture, providing ~230 µm thick diffusion zone without any compound layer. After nitriding all specimens were polished to a mirror-like finish ($R_a = 0.1 \mu\text{m}$) and coated with the commercial TiN/TiB₂ nanocomposite multilayer coating. Coating consisted of a primary TiN monolayer, a multilayer zone (TiN/Ti-B-N) with a lamella thickness of 85 nm and a top TiB₂ overcoat. TiN/TiB₂ coating with total thickness of ~2 µm and hardness of 3000 HV was deposited by a bipolar-pulsed glow discharge PACVD. Processing temperature was 530 °C and pressure 200 Pa.

In the case of PM cold work tool steel (PM-CW) three groups of vacuum heat treatment parameters were used and combined with the process of deep cryogenic treatment (Table 2). First group (A1) providing maximum hardness was quenched from high austenitizing temperature (1130 °C) and triple tempered at low tempering temperatures (520/520/490 °C). In order to increase fracture toughness but still maintain hardness above 64 HRC second group (A2) was austenitized at 1100 °C and tempered at 500 °C (500/500/470 °C). The last group (A3) was hardened from 1070 °C and triple tempered at increased tempering temperature (585/585/565 °C), thus providing high fracture toughness. In the cases when vacuum heat treatment was combined with deep cryogenic treatment—DCT (groups B1–B3), DCT was performed immediately after quenching and followed by a single 2 h tempering. DCT consisted of a controlled immersion of the test specimens in liquid nitrogen for 25 h (Table 2). After heat treatment specimens were mirror polished ($R_a = 0.10 \mu\text{m}$), sputter cleaned and coated. Investigation included three representative PVD coatings. These were monolayer TiAlN coating (~3300 HV), AlTiN/TiN multi-layer coating (~3500 HV) with lamellas thickness of ~50 nm and ~80 nm, respectively, and (Ti,Si)N nano-composite coating (~3800 HV). All three coatings were about 2 µm thick and deposited by magnetron sputtering process at the substrate temperature of ~450 °C. Details of the deposition process are provided in Reference [28,29].

The effect of substrate roughness on galling performance was evaluated by preparing A1 group of specimens with four different procedures; coarse grinding and polishing with a 20 µm industrial polishing paste (A1-1; $R_a = 0.5 \mu\text{m}$), coarse grinding and double polishing with 20 µm and 10 µm polishing paste (A1-2; $R_a = 0.3 \mu\text{m}$), fine grinding (A1-3; $R_a = 0.15 \mu\text{m}$) and polishing (A1-4; $R_a = 0.1 \mu\text{m}$). Afterwards specimens were coated with commercial TiN monolayer and W-doped DLC multilayer coating [30].

Table 2. Vacuum heat treatment and deep-cryogenic treatment parameters for P/M cold work tool steel.

Group	Austenitizing		Deep-Cryogenic Treatment		Tempering	
	Temp. [°C]	Time [min]	Temp. [°C]	Immersion Time [h]	Temp. [°C]	Time [h]
A1	1130	6	–	–	520/520/500	2/2/2
A2	1100	20	–	–	500/500/480	2/2/2
A3	1070	20	–	–	585/585/565	2/2/2
B1	1130	6	–196	25	520	2
B2	1100	20	–196	25	500	2
B3	1070	20	–196	25	585	2

2.3. Mechanical Properties

For each material CNPTB specimens [20] (Figure 1) were machined and used for further investigation. Fracture toughness was measured by pre-cracking CNPTB specimen under rotating-bending loading (400 N, 4500 cycles). After pre-cracking specimens were subjected to tensile load at the cross-head speed of 1.0 mm/min until fracture. Measuring the load at fracture (P) and diameter of the fractured area (d) fracture toughness is calculated according to the Equation (1) [31,32]. Details of the CNPTB specimen and fracture toughness measurement technique are given in Ref. [20]. For each group of treated specimens at least 12 samples were characterized in order to provide reliable results.

$$K_{Ic} = \frac{P}{d_0^{3/2}} \cdot \left(-1.27 + 1.72 \frac{d_0}{d} \right) \quad (1)$$

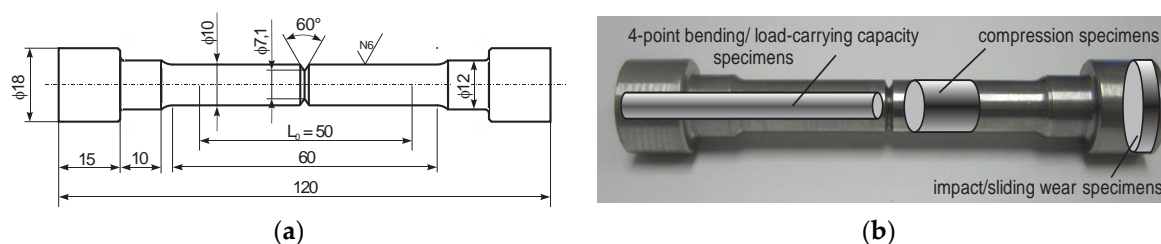


Figure 1. (a) Circumferentially notched and fatigue-pre-cracked tensile bar (CNPTB) specimen and (b) extraction of 4-point bending, load-carrying capacity, compression and sliding/impact wear test specimens.

Rockwell-C hardness measurements, performed circumferentially ($\times 3$) on each CNPTB specimen, were carried out on Willson-Rockwell B2000 machine (Buehler, Esslingen, Germany) and then average value calculated.

One half of the fractured CNPTB specimen was used to machine $\phi 10 \text{ mm} \times 12.5 \text{ mm}$ cylinder for compression test (Figure 1) and $\phi 18 \text{ mm} \times 8 \text{ mm}$ disc for sliding and impact wear testing. Compression tests were performed according to ASTM E9-09 standard [33] and used to determine yield strength, maximum compression strength and strain hardening exponent. Strain hardening exponent was defined between yield and maximum compression stress on a log-log plot of true stress-true strain. The other part of the fractured CNPTB specimen was used to prepare 4-point bending test specimen ($\phi 5 \text{ mm} \times 60 \text{ mm}$) or load-carrying capacity test specimens ($\phi 10 \text{ mm} \times 60 \text{ mm}$) (Figure 1). After high-speed machining, bending and load-carrying capacity test specimens were ground and polished ($R_a = 0.1 \mu\text{m}$). 4-point bending tests at room temperature were performed according to ASTM E290-09 standard [34], using support span of 40 mm and load span of 16 mm.

Effect of heat treatment on the machinability was analyzed by measuring surface roughness of as machined 4-point bending specimens. High-speed machining involved pre-turning with standard cutting inserts (Sandvik-Coromant DNMG11 R0.4, Sandviken, Sweden) at a cutting speed of 100 m/min,

depth of cut of 0.3 mm and feed rate of 0.12 mm/rev, followed by final turning (VBMT 16 04 cutting inserts) at the same cutting speed, depth of cut of 0.2 mm and feed rate of 0.08 mm/rev. Each specimen was machined with a new cutting insert and surface roughness analyzed (ISO 4287:1997 standard [35]) by Alicona InfiniteFocus G4 microscope (Alicona, Raaba, Austria).

2.4. Load-Carrying Capacity and Wear Testing

Load-carrying capacity was evaluated by load-scanning test rig, Figure 2a. The test configuration consists of two crossed cylinders (10 mm) which are sliding against each other at fixed speed, but progressive loading. Thus, each position of the wear scar corresponds to a unique load without any loading history [36]. In this investigation coated tool steel cylinder was loaded against polished WC cylinder ($R_a = 0.05 \mu\text{m}$, 2200 HV), using dry sliding conditions, room temperature, fixed sliding speed of 0.01 m/s and normal load in the range of 400–4000 N ($p_H = 2.8\text{--}6.1 \text{ GPa}$). Load-carrying capacity is determined by defining critical loads at which first cracks in the coating are observed and when coating starts to flake [4,36].

Sliding wear tests were done under dry sliding conditions using ball on disc contact configuration and reciprocating sliding (Figure 2b). Polished 20 mm diameter Al_2O_3 ball ($R_a = 0.05 \mu\text{m}$) was used as a counter material in order to simulate abrasive wear mode and focus all the wear on the investigated disc material. Test were done under normal room conditions (RT and 45% RH) and elevated temperature of 150 °C applying different contact conditions; loads corresponding to contact pressure between 800 and 1300 MPa and sliding speeds between 0.01 and 0.1 m/s, obtained by changing oscillating frequency from 1 to 15 Hz. All tests were performed up to the total sliding distance of 100 m (up to two hours), with the average coefficient of friction being analyzed and wear volume measured using 3D confocal microscope.

Impact wear tests were performed on servo hydraulic fatigue testing machine, with the coated disc being repetitively impacted against a WC ball ($\phi 32 \text{ mm}$; Figure 2c). Testing machine is position controlled during testing, which includes continuous monitoring of the impact force. Impact wear tests were performed at the frequency of 30 Hz, initial impacting distance of 0.5 mm and maximum impacting load of 5.5 kN ($p_H = 3.5 \text{ GPa}$). New WC ball was used for each test and testing specimens cleaned with ethanol. Adhesive wear of the WC ball was prevented by applying a thin layer of lithium grease on the disc surface.

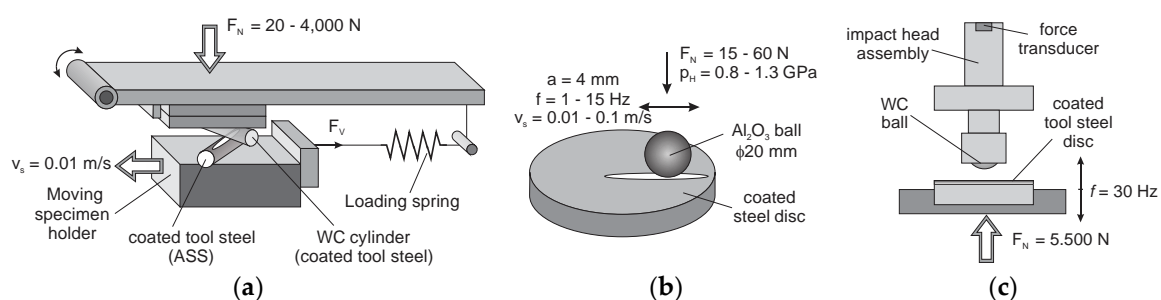


Figure 2. Load-carrying capacity and wear testing setups; (a) load scanner, (b) reciprocating sliding wear test, (c) impact wear test.

Effect of substrate roughness and surface quality on resistance against galling was also evaluated by a load-scanning test rig (Figure 2a). In this case tempered austenitic stainless steel (ASS) cylinder (AISI 304, 335 HV, $R_a = 0.2 \mu\text{m}$, $\phi 10 \text{ mm}$) was used as a moving counter cylinder. Galling tests were performed dry, using sliding speed of 0.01 m/s and normal load from 20 to 1300 N. Results were then evaluated by analyzing wear tracks after sliding and determining critical loads for galling initiation and gross galling formation [36,37].

3. Results

3.1. Tool Steel Substrate Properties Correlation

Diagram displaying fracture toughness and hardness of vacuum heat treated AISI H11 type hot work tool steel as depending on the tempering and austenitizing temperature is shown in Figure 3. Fracture toughness obtained by hardening from 1000 °C followed by double tempering at 630 °C was 87 MPa√m. It was reduced to less than 30 MPa√m by reducing tempering temperature to 550 °C. Hardness, on the other hand, increased from 40 HRC to almost 50 HRC. Further hardness increase is provided by increased Si content and austenitizing temperature. In the case of low Si content, increase in austenitizing temperature to 1030 °C results in about 5% higher hardness (up to 52 HRC) and for high Si content even more, especially at low tempering temperatures, up to 54 HRC. However, for low Si hot work tool steel increase in austenitizing temperature also provided higher fracture toughness, being between 45 and 115 MPa√m, while for high Si content fracture toughness has been reduced at elevated austenitizing temperature, ranging between 25 and 80 MPa√m, as shown in Figure 3.

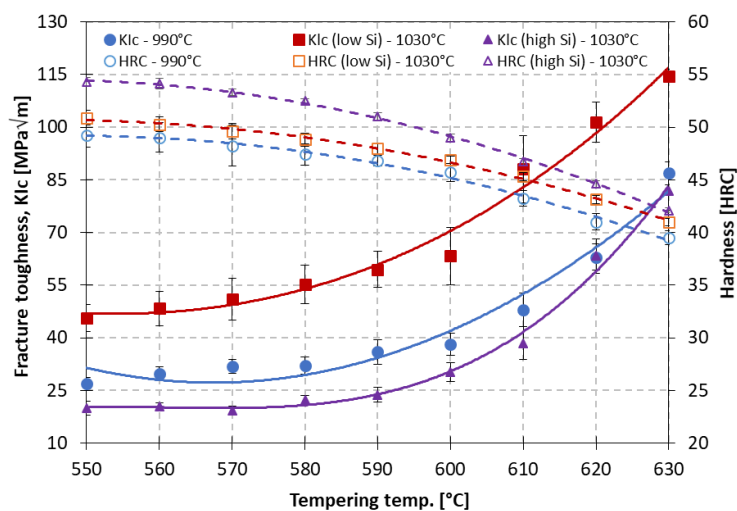


Figure 3. Effect of Si content and heat treatment temperatures on fracture toughness and hardness of AISI H11 hot work tool steel.

Yield and ultimate compression strength of the investigated hot work tool steel (AISI H11) are between 1200 and 1850 MPa, and 1450 and 2130 MPa, respectively. Similar to hardness, ultimate compression strength and yield strength are increasing when increasing austenitizing temperature (for 5%) and Si content, but decreasing with tempering temperature, as shown in Figure 4a. On the other hand, material ductility being analyzed by measuring strain hardening exponent was found mainly independent on the austenitizing and tempering temperature. For the tempering temperatures up to 610 °C it shows more or less constant value, 0.45 for low Si content and 0.4 for high Si content.

In the case of bending test, maximum and yield strength at the austenitizing temperature of 990 °C changed from 1860 and 3260 MPa to 2600 and 4550 MPa, respectively, when reducing tempering temperature from 630 to 550 °C. Further increase was obtained by increasing austenitizing temperature to 1030 °C. In this case and low Si content, yield and maximum bending strength reached peak values (tempering at 550 °C) of 2700 and 4780 MPa, respectively, and even up to 2800 and 4950 MPa, respectively, for high Si content (Figure 4b).

When analyzing correlations, strong correlation between hardness and strength of tool steel substrate has been observed. In agreement with well-established correlations [38,39] compression and bending strength increase linearly with hardness, but dropping digressively with fracture toughness,

as shown in Figure 5. On the other hand, strain hardening exponent has no direct correlation with hardness but it shows rising trend with increased fracture toughness (Figure 6).

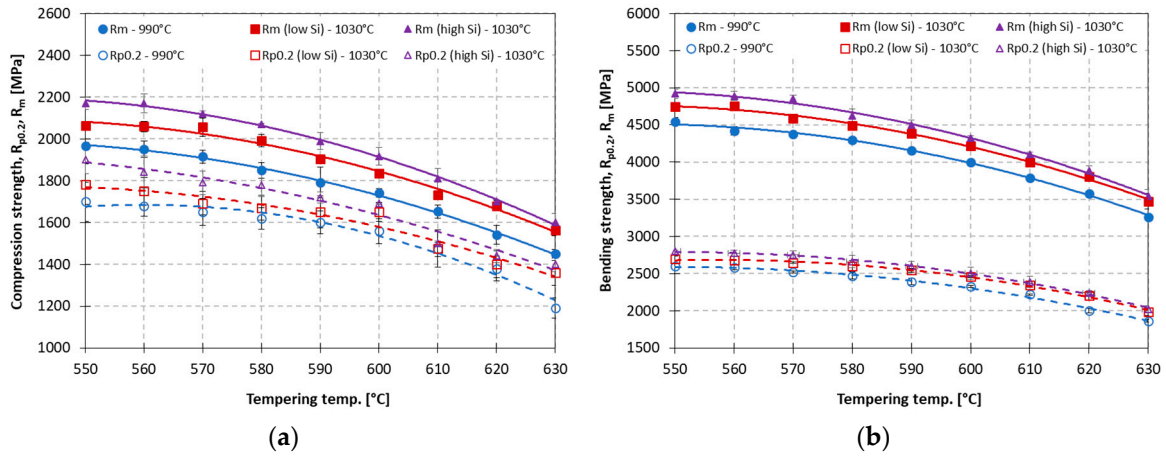


Figure 4. (a) Compression and (b) bending strength tempering diagram.

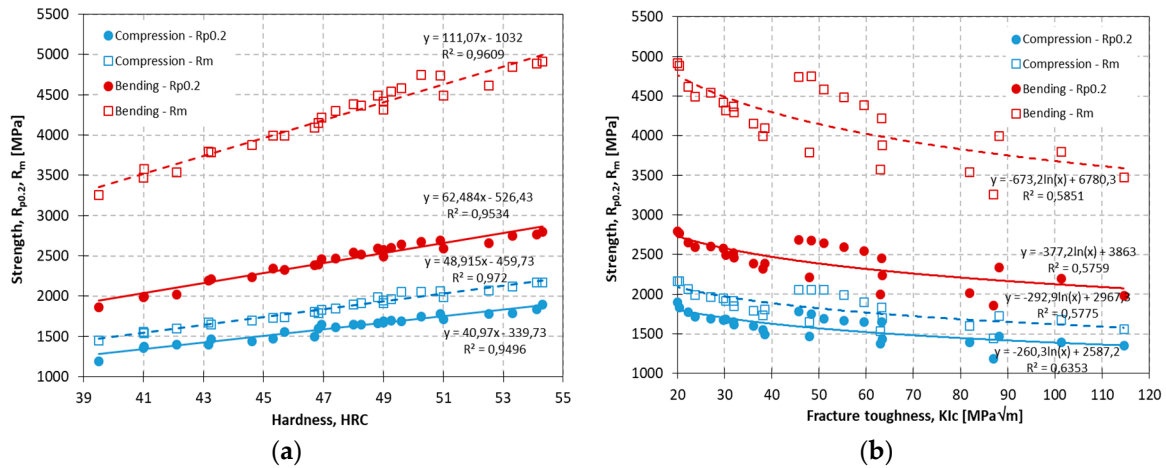


Figure 5. Strength vs. (a) hardness and (b) fracture toughness correlation.

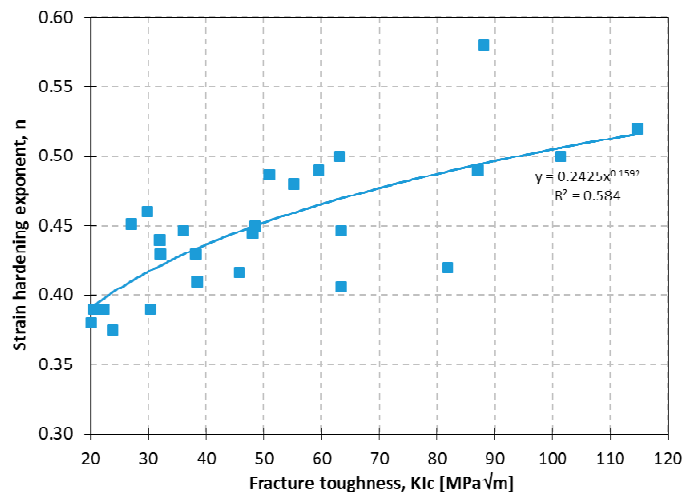


Figure 6. Strain hardening exponent vs. fracture toughness correlation.

Surface roughness analysis of machined 4-point bending and load-carrying capacity specimens revealed deteriorated surface quality with higher average roughness and intensified tearing component

when increasing tempering as well as austenitizing temperature [39]. As shown in Figure 7, lower average roughness values (R_a), lower kurtosis (R_{ku}) representing less sharp surface profile and zero skewness (R_{sk}) indicating symmetric profile, with all indicating improved machinability and better surface quality of tool steel substrate, are obtained when increasing hardness (above 45 HRC) and having fracture toughness below 60 $\text{MPa}\sqrt{\text{m}}$. However, when material becomes too hard, above 50 HRC or too tough ($>80 \text{MPa}\sqrt{\text{m}}$) surface quality quickly deteriorates (Figure 7) and becomes too rough for coating deposition [40].

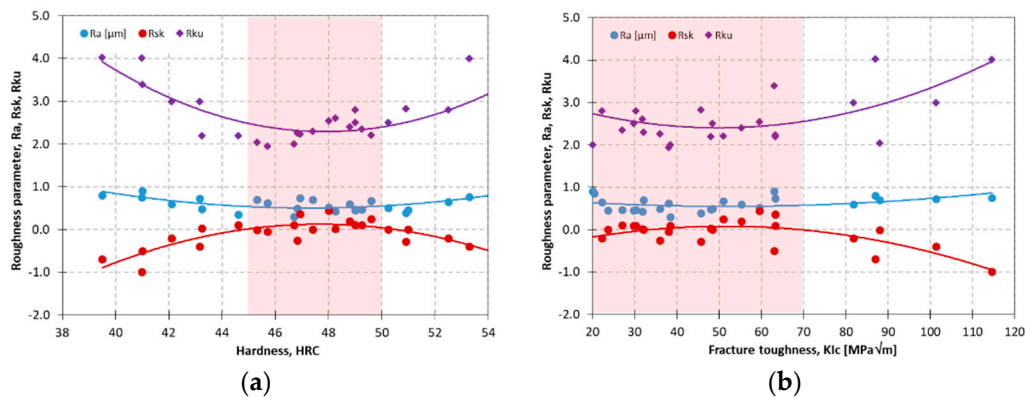


Figure 7. Effect of (a) hardness and (b) fracture toughness on surface quality.

In terms of tribological properties, coefficient of friction for AISI H11 tool steel was found largely independent on the austenitizing and tempering temperature, displaying average value of about 0.75, which is well in agreement with many tribological investigations on tool steels. On the other hand, wear volume was found to increase with tempering temperature and being dependent also on austenitizing temperature. Furthermore, the form and rate of increase was dependent on the contact conditions used, as shown in Figure 8. In the case of low load-low sliding speed and high load-low sliding speed (Figure 8a) conditions wear volume shows linear increase with tempering temperature, with the higher austenitizing temperature giving faster increase rate and higher wear, especially for high loads. By increasing the sliding speed (low load-high sliding speed and high load-high sliding speed—Figure 8b) effect of austenitizing temperature on wear has been reversed. In these cases, wear shows exponential increase with tempering temperature but drop in values for higher austenitizing temperature, which is more pronounced in the low tempering range (Figure 8b). Furthermore, the best wear resistance and the lowest wear was observed for mid-tempering range between 570 and 590 °C. This indicates that for low sliding speeds higher fracture toughness obtained by lower austenitizing temperature is dominating over hardness, while for high sliding speeds hardness prevails.

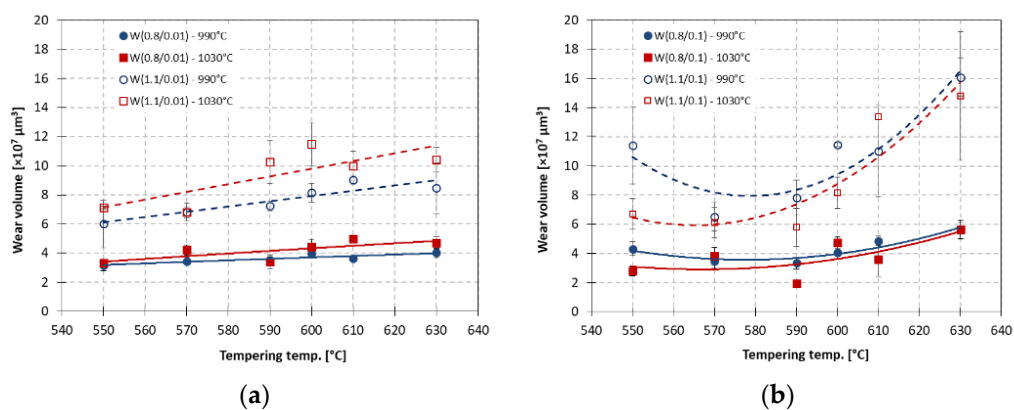


Figure 8. Wear of AISI H11 tool steel as a function of heat treatment temperatures; (a) low sliding speed and (b) high sliding speed case.

When it comes to friction under abrasive wear conditions, steady-state coefficient of friction for tool steel was found largely unaffected by fracture toughness and hardness when operating within working hardness range (42–52 HRC). On the other hand, as shown in Figure 9, wear volume and wear rate, defined as wear volume divided by load and sliding distance show direct dependency on hardness and fracture toughness. Under the abrasive wear conditions wear rate increases with fracture toughness and is reduced with hardness, with the hardness being found as the most influencing parameter. For the best abrasive wear resistance tool steel hardness should be above 48 HRC (strength above 1900 MPa) and fracture toughness below 55 MPa \sqrt{m} , although not too low (Figure 9).

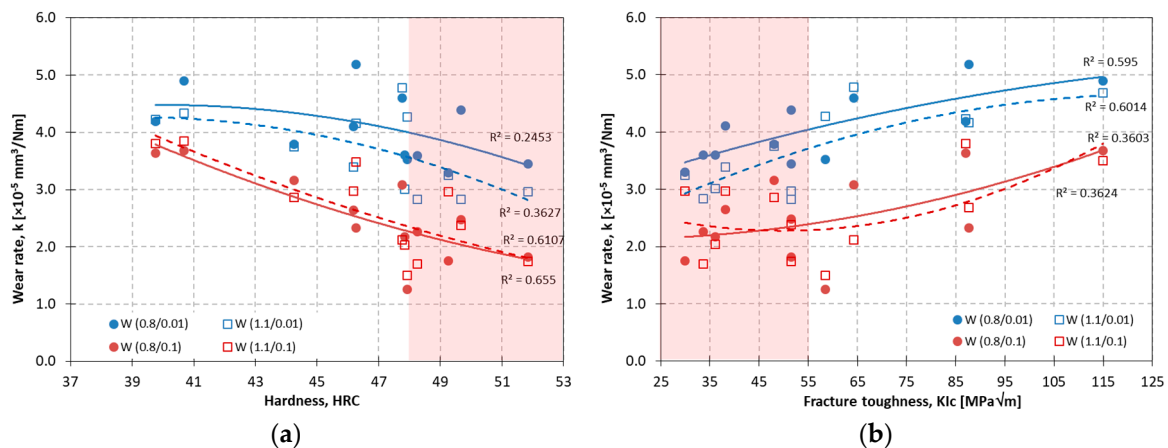


Figure 9. Effect of (a) hardness and (b) fracture toughness on hot work tool steel wear resistance.

3.2. Thermo-Chemical Treatment vs. Coating

Based on Archard law [41] abrasive wear resistance of materials is in general dependent on their hardness. Hardness increase and thus better wear resistance of steels can be achieved by increasing austenitizing and decreasing tempering temperature [42]. However, even higher surface hardness is provided by thermo-chemical processes, i.e., nitriding and deposition of wear resistant coatings [12]. As shown in Figure 10 plasma nitriding in 5% N₂:95% H₂ gas mixture, providing nitrided surface without compound layer and a hardness of 1100 HV_{0.05} reduces wear of hot work tool steel by about 25%. However, although operating under abrasive wear mode and wear being concentrated within the nitride zone of just 250 μm [4] steel core microstructure and properties, especially hardness and fracture toughness play an important role in terms of surface wear resistance. For lower austenitizing temperature with the hardness in the range of 47–50 HRC and fracture toughness above 35 MPa \sqrt{m} wear rate of nitrided surface increases as the hardness is reduced (higher tempering temperature). On the other hand, increase in austenitizing temperature, providing higher core hardness (51–53 HRC) but much lower toughness (<30 MPa \sqrt{m} ; Figure 3) resulted in about 30% higher wear of the investigated AISI H11 tool steel, both at room and high temperature sliding. In this case wear resistance of plasma nitrided tool steel has been found more or less unaffected by core hardness, but mainly defined by reduced fracture toughness, which is further escalated by nitriding and formation of hard brittle surface zone [43].

Although nitriding improves wear resistance of metallic surfaces [44] it cannot match wear resistance provided by PVD and CVD coatings. As shown in Figure 10, coating of tool steel by hard protective TiN/TiB₂ coating can improve surface wear resistance by two orders of magnitude. Furthermore, when load is carried entirely by the top coating and substrate deformation is within elastic range wear rate of the coated surface becomes independent on the substrate preparation and properties, including heat treatment temperatures and/or plasma nitriding used [4].

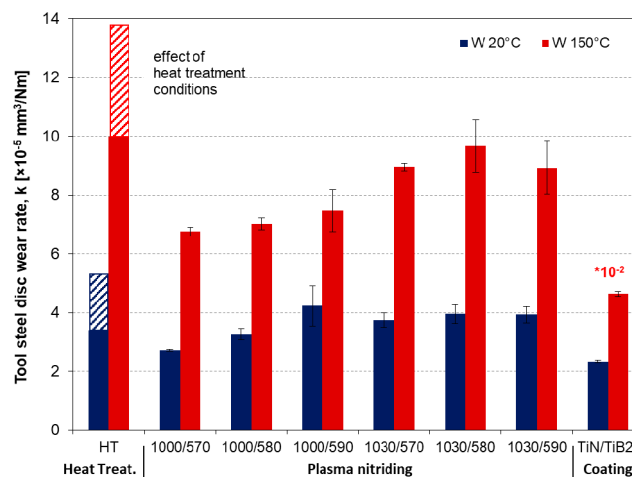


Figure 10. Effect of heat treatment, plasma nitriding and coating deposition on wear resistance of hot work tool steel.

In the case of coated surface load-carrying capacity is the primary requirement. As shown in Figure 11, it doesn't depend just on core hardness but also on the subsurface properties determined by the eventual thermo-chemical process [4]. In the case of plasma nitriding, producing few microns thick compound layer (25% N₂:75% H₂) on the hot work tool steel surface, increase in tempering temperature and corresponding drop in core hardness of less than 5 HRC led to about 30% lower critical loads for TiN/TiB₂ coating cracking and flaking or spallation. Even though compound layer may provide additional load support [45], it is quite brittle and thus its cracking resistance dependent on the core hardness. Any crack starting in the compound layer will propagate directly into the substrate but mainly into and through the top coating [46], Figure 12. By avoiding formation (5% N₂:95% H₂) or removing the intermediate compound layer load-carrying capacity drops further. However, it is influenced by the combined effect of fracture toughness and core hardness. For low hardness values (50 HRC) and fracture toughness above 30 MPa√m (austenitizing @1000 °C) increase in fracture toughness obtained by higher tempering temperatures prevails over the reduction in core hardness providing better coating resistance to cracking and load-carrying capacity. Positive effect of core fracture toughness is present also for lower toughness values (<30 MPa√m) but it fades away as soon as core hardness drops to about 50 HRC, as shown in Figure 11.

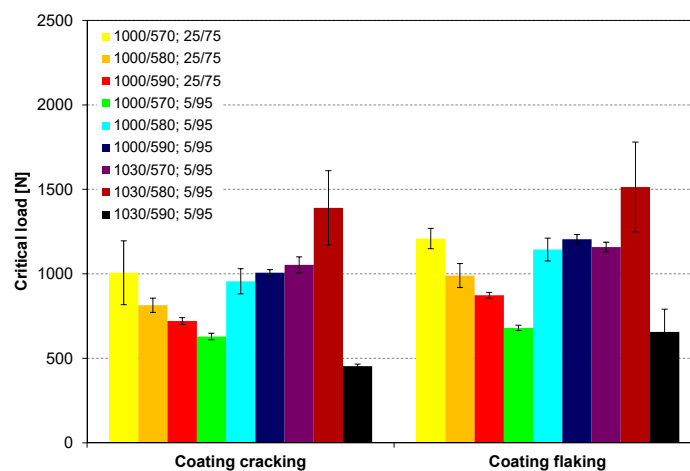


Figure 11. Dependency of load-carrying capacity on substrate heat treatment and plasma nitriding conditions [4]. Reprinted with permission from [4]. Copyright 2015 Elsevier.

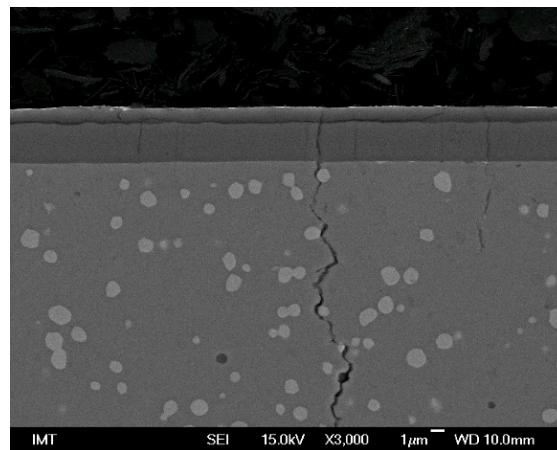


Figure 12. Crack pattern in TiN/TiB₂ coated and plasma nitrided hot work tool steel with intermediate compound layer.

3.3. Effect of Substrate Hardness and Fracture Toughness on Coating Performance

Coatings represent only one part of the coated system and require proper substrate giving sufficient support. Thus, beside coating type its properties and performance greatly depend on the substrate, mainly its hardness and fracture toughness. Hardness provides resistance to plastic deformation while fracture toughness is responsible for hindering crack initiation and propagation. As shown in Table 3, by combining different heat treatment parameters (tempering and austenitizing temperature) with eventual deep cryogenic treatment different combinations of fracture toughness and hardness for cold work tool steel can be obtained.

Table 3. Fracture toughness and hardness of P/M cold work tool steel using different heat treatment procedures.

Substrate Treatment	Fracture Toughness K_{Ic} [MPa \sqrt{m}]	Hardness HRC	K_{Ic}/HRC
A1	6.1 ± 1.2	65.8 ± 0.2	0.09
A2	10.2 ± 2.0	64.0 ± 0.2	0.159
A3	12.7 ± 0.7	59.3 ± 0.1	0.214
B1	10.4 ± 0.8	65.0 ± 0.3	0.160
B2	12.4 ± 0.7	64.2 ± 0.4	0.193
B3	14.2 ± 0.4	59.5 ± 0.1	0.239

Load-carrying capacity results for three different coatings (monolayer, multilayer, nano-composite) obtained for different core hardness vs. fracture toughness values are shown in Figure 13. In the case of a TiAlN monolayer coating deposited on the hardest tool steel substrate (66 HRC; Group A1) first signs of coating cracking are observed at the critical load of about 3.1 kN. Increase in fracture toughness from 6 to 10 MPa \sqrt{m} at the same time resulting in reduced substrate hardness (66→64 HRC; Group A2) leads to loss in load-carrying capacity, reducing critical load for coating cracking for about 10%, down to 2.8 kN. Further drop in hardness (60 HRC; Group A3), in spite of providing high fracture toughness values results in additional 10% drop in load-carrying capacity ($L_C < 2.5$ kN). However, when maintaining high hardness level (above 65 HRC) any increase in fracture toughness, obtained by combining conventional heat treatment with deep cryogenic treatment [17,27] will provide better crack initiation and propagation resistance and thus higher load-carrying capacity (Group B1).

In the case of AlTiN/TiN multilayer coating with improved cracking resistance, substrate hardness above or equal 64 HRC provides comparable load-carrying capacity, regardless of the K_{Ic}/HRC ratio and level of the fracture toughness obtained (Figure 13). However, with the drop in substrate hardness below 60 HRC (Group A3) critical loads for the beginning of coating cracking are reduced, indicating about 20% lower load-carrying capacity. This time increase in fracture toughness (Group B3)

provides some load-carrying capacity improvement, although not reaching the same level as with the harder substrates.

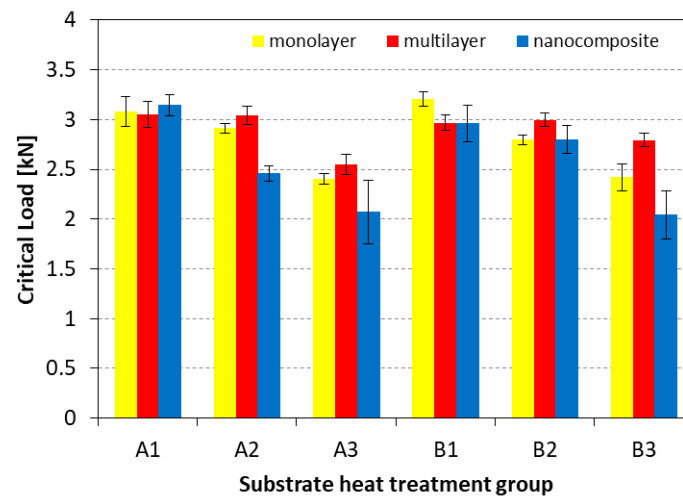


Figure 13. Load-carrying capacity of different coating types as a function of substrate heat treatment and properties.

The most marked effect of substrate properties on load-carrying capacity is found for the most brittle and hardest (Ti,Si)N nano-composite coating. Again, the best load-carrying capacity is provided by the hardest substrate, but very low for too soft one, irrespectively of the fracture toughness level obtained. On the other hand, fracture toughness becomes important for the intermediate working hardness values, as shown in Figure 13. Combination of high fracture toughness ($>12 \text{ MPa}\sqrt{\text{m}}$; Group B2) and working hardness of about 64 HRC guarantees load-carrying capacity similar to hardest substrates but at greatly improved fatigue resistance.

Another coating property, altered by substrate properties is its impact wear resistance. In agreement with high load-carrying capacity the best impact wear resistance for different types of hard coatings is achieved when applied on steel substrate with the highest hardness (Group A1; Figure 14). In this case coatings are removed through abrasive wear mechanism, without any evident coating delamination or cracking. Even the smallest drop in hardness, even though accompanied by increased fracture toughness (Groups B1 and A2) leads to increased coating impact wear and beginning of coating delamination. However, if hardness of about 64 HRC is paired with the fracture toughness above $12 \text{ MPa}\sqrt{\text{m}}$ (Group B2) coating impact wear can be reduced for up to 30%, closely matching harder but more brittle substrate case. Improved fracture toughness retards crack initiation and propagation while high hardness guarantees high load support. Further rise in fracture toughness, meaning drop in hardness below 60 HRC (Group A3 and B3) has clear negative effect. Low load-carrying capacity of the steel substrate results in excessive deformations and thus in high impact wear of the coating. However, for the most brittle and the hardest coatings (i.e., (Ti,Si)N) substrate hardness is found as the dominant factor in terms of impact wear resistance. In this case, the steel substrate with the highest hardness is the most suitable (66 HRC; Group A1). Use of any softer substrate results in coating cracking and flaking with wear exceeding coating thickness (Figure 14).

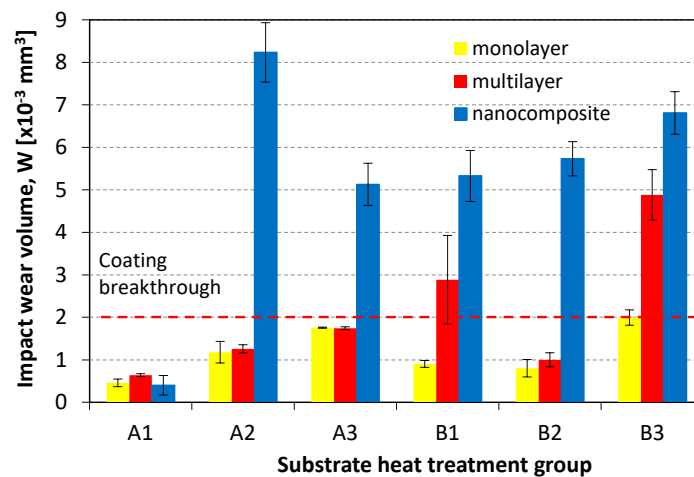


Figure 14. Impact wear volume for different coating types and substrate pre-treatments.

3.4. Effect of Substrate Roughness

If tool is coated its galling resistance depends on the material to be formed and coating type, as well as on the substrate roughness and any additional surface treatment, i.e., post-polishing [25,47]. In the case of hard nitride-based coatings, i.e., TiN, which generally show lower galling resistance than tool steels [48], substrate roughness is even more important. For rough, coarse ground substrates (A1-1 & A1-2) coating gives higher friction (0.4) and about 25% lower galling resistance as indicated by reduced critical loads for stainless steel transfer, as compared to uncoated tool steel (Figure 15). However, by reducing roughness of the substrate (A1-3 and A1-4) coated surface provides comparable resistance to galling and material transfer. Even more, when post-polished (A1-3 + post-polishing) to Ra values of 0.1, use of coated surface can provide up to two times higher resistance to galling. On the other hand, low friction and excellent galling resistance against ASS are obtained by low-friction DLC coating, regardless of the substrate roughness and post-polishing procedure (Figure 15), with the critical loads for galling exceeding 1 kN even under dry sliding [48].

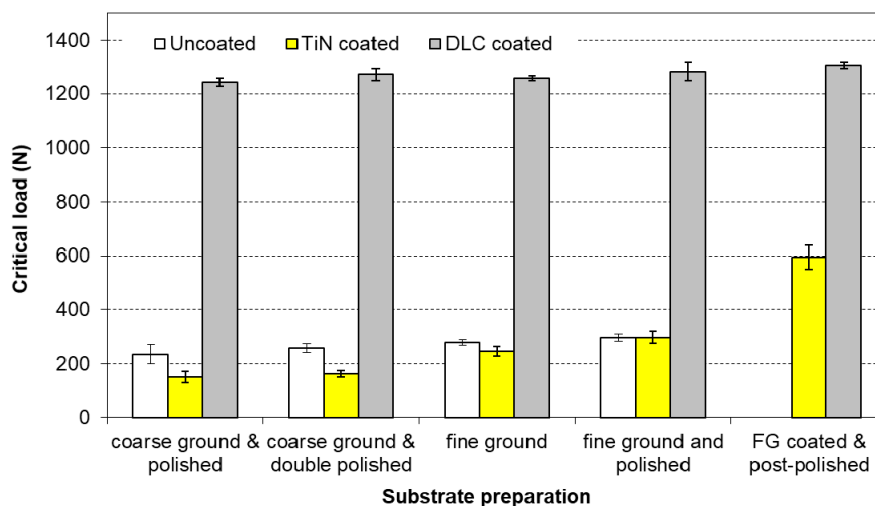


Figure 15. Effect of substrate roughness and post-polishing of coated surface on galling resistance.

4. Conclusions

Effect of steel substrate properties on coating performance can be summarized in the following conclusions:

- Yield and maximum compression and bending strength of the tool steel substrate show rising linear dependency on hardness and reduced trend with fracture toughness. On the other hand, strain hardening exponent has no direct correlation with hardness but shows rising trend with increased fracture toughness.
- Thermo-chemical treatment, i.e., plasma nitriding, provides up to 25% better tool steel wear resistance. However, even when plasma nitrided wear resistance depends on combination of fracture toughness and core hardness. Higher hardness of the core material improves abrasive wear resistance of the surface, but sufficient fracture toughness level needs to be provided. On the other hand, hard wear-resistant coatings outperform all other surface engineering techniques, providing up to two orders of magnitude better tool abrasive wear resistance.
- In the case of coated applications steel substrate must provide sufficient load-carrying capacity and support for the coating. A compound layer can be used as an additional interlayer, but its brittleness results in accelerated coating cracking as the core hardness is reduced. Even for cases without compound layer, high level of steel core hardness (above 50 HRC) is mandatory in order to provide good load support for the top coating. However, high hardness must also be supported by proper level of the fracture toughness (above 30 MPa√m).
- Surface roughness and topography have major influence on galling resistance in forming, with smoother surfaces and plateau-like topography providing better results. This is further escalated for coated surfaces, where galling resistance depends on substrate roughness level, coating type and material to be formed. In the case of typical hard ceramic coatings post-polishing of the coated surface and use of smoothed substrate gives about 2 times better galling resistance. On the other hand, for carbon-based low friction coatings post-polishing and roughness of the substrate have very limited effect on the tool resistance against galling and work material transfer.

Workshop practice recommendations:

- Abrasive wear resistance as well as surface quality of hot work tool steel mainly depend on hardness but also on fracture toughness. Good machinability and the best surface quality are obtained when hardness is between 45 and 50 HRC, and high abrasive wear resistance for hardness above 48 HRC. Fracture toughness, however, should be below 55–60 MPa√m to get best performance. On the other hand, coefficient of friction is independent on heat treatment parameters and mainly depends on contact conditions.
- In the case of cold work tool steel, hardness of over 64 HRC is required to obtain sufficient load-carrying capacity of the coated surface, regardless of the coating type used. However, required level of the fracture toughness is dependent also on the coating type. In the case of monolayer coatings, the main parameter is hardness of the substrate with higher the better. For typical multilayer coatings, having improved resistance to crack initiation and propagation, substrate hardness of about 64 HRC is sufficient and high fracture toughness only required at low hardness. However, for very brittle coatings combination of working hardness and high fracture toughness (above 10 MPa√m) gives superior results.
- Substrate hardness is the most influential parameter also when it comes to impact wear resistance, which is true for different types of hard coatings. However, except for very brittle coatings fracture toughness of the steel substrate should be above 12 MPa√m and hardness in the range of 64–65 HRC, thus providing combination of high load-carrying capacity, good fatigue properties and superior resistance against impact wear.

Author Contributions: Conceptualization, B.P.; methodology, B.P.; validation, B.P., M.S. and B.Ž.; formal analysis, M.S. and B.Ž.; investigation, M.S. and A.G.; writing—original draft preparation, B.P.; supervision, B.P. All authors have read and agreed to the published version of the manuscript.

Funding: This research was funded by Slovenian Research Agency (research core funding No. P2-0050 and research project L2-9211).

Acknowledgments: Authors would like to acknowledge help from Miha Čekada from Institute Jozef Stefan for the deposition and supply of coatings.

Conflicts of Interest: The authors declare no conflict of interest. The funders had no role in the design of the study; in the collection, analyses, or interpretation of data; in the writing of the manuscript, or in the decision to publish the results.

References

1. Behrens, B.-A.; Doege, E.; Reinsch, S.; Telkamp, K.; Daehndel, H.; Specker, A. Precision forging processes for high-duty automotive components. *J. Mater. Process. Technol.* **2007**, *185*, 139–146. [[CrossRef](#)]
2. Podgornik, B.; Leskovšek, V. Experimental evaluation of tool and high-speed steel properties using multi-functional K_{IC} -test specimen. *Steel Res. Int.* **2013**, *84*, 1294–1301. [[CrossRef](#)]
3. Pérez, M.; Belzunce, F.J. The effect of deep cryogenic treatments on the mechanical properties of an AISI H13 steel. *Mater. Sci. Eng. A* **2015**, *624*, 32–40. [[CrossRef](#)]
4. Podgornik, B.; Leskovšek, V.; Tehovnik, F.; Burja, J. Vacuum heat treatment optimization for improved load carrying capacity and wear properties of surface engineered hot work tool steel. *Surf. Coat. Technol.* **2015**, *261*, 253–261. [[CrossRef](#)]
5. Shanbhag, V.V.; Rolfe, B.F.; Griffin, J.M.; Arunachalam, N.; Pereira, M.P. Understanding galling wear initiation and progression using force and acoustic emissions sensors. *Wear* **2019**, 436–437, 202991. [[CrossRef](#)]
6. Mellouli, D.; Haddar, N.; Köster, A.; Ayedi, H.F. Hardness effect on thermal fatigue damage of hot-working tool steel. *Eng. Fail. Anal.* **2014**, *45*, 85–95. [[CrossRef](#)]
7. Norström, L.-Å.; Svensson, M.; Öhrberg, N. Thermal-fatigue behaviour of hot-work tool steels. *Met. Technol.* **1981**, *8*, 376–381. [[CrossRef](#)]
8. Leskovšek, V.; Šuštaršič, B.; Jutriša, G. The influence of austenitizing and tempering temperature on the hardness and fracture toughness of hot-worked H11 tool steel. *J. Mater. Process. Technol.* **2006**, *178*, 328–334. [[CrossRef](#)]
9. Shirgaokar, M. Technology to Improve Competitiveness in Warm and Hot Forging: Increasing Die Life and Material Utilization. Ph.D. Thesis, Ohio State University, Columbus, OH, USA, 2008.
10. Eller, T.; Greve, L.; Andres, M.; Medricky, M.; Meinders, V.T.; Boogaard, A.V.D.; Boogaard, A.H.V.D. Determination of strain hardening parameters of tailor hardened boron steel up to high strains using inverse FEM optimization and strain field matching. *J. Mater. Process. Technol.* **2016**, *228*, 43–58. [[CrossRef](#)]
11. Roberts, G.A.; Kennedy, R.; Krauss, G. *Tool Steels*, 5th ed.; ASM International: Materials Park, OH, USA, 1998.
12. Podgornik, B.; Leskovšek, V. Wear mechanisms and surface engineering of forming tools. *Mater. Tehnol.* **2015**, *49*, 313–324. [[CrossRef](#)]
13. Eser, A.; Broeckmann, C.; Sirmsir, C. Multiscale modeling of tempering of AISI H13 hot-work tool steel—Part 1: Prediction of microstructure evolution and coupling with mechanical properties. *Comput. Mater. Sci.* **2016**, *113*, 280–291. [[CrossRef](#)]
14. Li, J.-Y.; Chen, Y.-L.; Huo, J.-H. Mechanism of improvement on strength and toughness of H13 die steel by nitrogen. *Mater. Sci. Eng. A* **2015**, *640*, 16–23. [[CrossRef](#)]
15. Ramezani, M.; Pasang, T.; Chen, Z.; Neitzert, T.; Au, D. Evaluation of carbon diffusion in heat treatment of H13 tool steel under different atmospheric conditions. *J. Mater. Res. Technol.* **2015**, *4*, 114–125. [[CrossRef](#)]
16. Lerchbacher, C.; Zinner, S.; Leitner, H. Direct or indirect: Influence of type of retained austenite decomposition during tempering on the toughness of a hot-work tool steel. *Mater. Sci. Eng. A* **2013**, *564*, 163–168. [[CrossRef](#)]
17. Podgornik, B.; Paulin, I.; Zajec, B.; Jacobson, S.; Leskovšek, V. Deep cryogenic treatment of tool steels. *J. Mater. Process. Technol.* **2016**, *229*, 398–406. [[CrossRef](#)]
18. Telasang, G.; Majumdar, J.D.; Padmanabham, G.; Manna, I. Structure–property correlation in laser surface treated AISI H13 tool steel for improved mechanical properties. *Mater. Sci. Eng. A* **2014**, *599*, 255–267. [[CrossRef](#)]
19. Dossett, J.L.; Totten, G.E. *ASM Handbook Volume 4A: Steel Heat Treating Fundamental and Processes*; ASM International: Materials Park, OH, USA, 2013.
20. Podgornik, B.; Žužek, B.; Leskovšek, V. Experimental evaluation of tool steel fracture toughness using circumferentially notched and precracked tension bar specimen. *Mater. Perform. Charact.* **2014**, *3*, 20130045. [[CrossRef](#)]

21. Groche, P.; Christiany, M. Evaluation of the potential of tool materials for the cold forming of advanced high strength steels. *Wear* **2013**, *302*, 1279–1285. [[CrossRef](#)]
22. Leskovšek, V.; Podgornik, B. Vacuum heat treatment, deep cryogenic treatment and simultaneous pulse plasma nitriding and tempering of P/M S390MC steel. *Mater. Sci. Eng. A* **2012**, *531*, 119–129. [[CrossRef](#)]
23. Podgornik, B.; Leskovšek, V.; Arh, B. The effect of heat treatment on the mechanical, tribological and load-carrying properties of PACVD-coated tool steel. *Surf. Coat. Technol.* **2013**, *232*, 528–534. [[CrossRef](#)]
24. Caliskan, H.; Panjan, P.; Kurbanoglu, C. 3.16 hard coatings on cutting tools and surface finish. In *Comprehensive Materials Finishing*; Hashmi, M.S.J., Ed.; Elsevier: Oxford, UK, 2017; pp. 230–242.
25. Podgornik, B.; Jerina, J. Surface topography effect on galling resistance of coated and uncoated tool steel. *Surf. Coat. Technol.* **2012**, *206*, 2792–2800. [[CrossRef](#)]
26. Podgornik, B.; Zajec, B.; Bay, N.O.; Vižintin, J. Application of hard coatings for blanking and piercing tools. *Wear* **2011**, *270*, 850–856. [[CrossRef](#)]
27. Podgornik, B.; Sedlaček, M.; Čekada, M.; Jacobson, S.; Zajec, B. Impact of fracture toughness on surface properties of PVD coated cold work tool steel. *Surf. Coat. Technol.* **2015**, *277*, 144–150. [[CrossRef](#)]
28. Miletić, A.; Panjan, P.; Skoric, B.; Čekada, M.; Dražić, G.; Kovac, J. Microstructure and mechanical properties of nanostructured Ti–Al–Si–N coatings deposited by magnetron sputtering. *Surf. Coat. Technol.* **2014**, *241*, 105–111. [[CrossRef](#)]
29. Panjan, M.; Gunde, M.K.; Panjan, P.; Čekada, M. Designing the color of AlTiN hard coating through interference effect. *Surf. Coat. Technol.* **2014**, *254*, 65–72. [[CrossRef](#)]
30. Podgornik, B.; Hogmark, S.; Sandberg, O.; Leskovšek, V. Wear resistance and anti-sticking properties of duplex treated forming tool steel. *Wear* **2003**, *254*, 1113–1121. [[CrossRef](#)]
31. Wei, S.; Zhao, T.; Gao, D.; Liu, D.; Li, P.; Qui, X. Fracture toughness measurement by cylindrical specimen with ring-shaped crack. *Eng. Fract. Mech.* **1982**, *16*, 69–82.
32. Gdoutos, E. *Fracture Mechanics Criteria and Applications*; Kluwer Academic Publishers: London, UK, 1990.
33. *ASTM E9-09 Standard Test Methods of Compression Testing of Metallic Materials at Room Temperature*; ASTM International: West Conshohocken, PA, USA, 2009.
34. *ASTM E290-09 Standard Test Methods for Bend Testing of Material for Ductility*; ASTM International: West Conshohocken, PA, USA, 2009.
35. *ISO 4287:1997 Geometrical Product Specifications (GPS)—Surface Texture: Profile Method—Terms, Definitions and Surface Texture Parameters*; International Organization for Standardization: Geneva, Switzerland, 1997.
36. Podgornik, B.; Hogmark, S.; Pezdinrik, J. Comparison between different test methods for evaluation of galling properties of surface engineered tool surfaces. *Wear* **2004**, *257*, 843–851. [[CrossRef](#)]
37. Podgornik, B.; Kafexhiu, F.; Nevosad, A.; Badisch, E. Influence of surface roughness and phosphate coating on galling resistance of medium-grade carbon steel. *Wear* **2020**, *446–447*, 203180. [[CrossRef](#)]
38. Pavlina, E.J.; Van Tyne, C.; Van Tyne, C. Correlation of yield strength and tensile strength with hardness for steels. *J. Mater. Eng. Perform.* **2008**, *17*, 888–893. [[CrossRef](#)]
39. Podgornik, B.; Puš, G.; Žužek, B.; Leskovšek, V.; Godec, M. Heat treatment optimization and properties correlation for H11-type hot-work tool steel. *Met. Mater. Trans. A* **2017**, *49*, 455–462. [[CrossRef](#)]
40. Wiklund, U.; Gunnars, J.; Hogmark, S. Influence of residual stresses on fracture and delamination of thin hard coatings. *Wear* **1999**, *232*, 262–269. [[CrossRef](#)]
41. Zmitrowicz, A. Wear patterns and laws of wear—A review. *J. Theor. Appl. Mech.* **2006**, *44*, 219–253.
42. Podgornik, B. Fracture toughness and wear resistance of hot work tool steel related to heat treatment conditions. In *Proceedings of the National Conference on Vacuum Heat Treatment and Heat Treatment of Tools*, Puchov, Slovakia, 20–21 November 2018; p. 10.
43. Fernandes, F.; Heck, S.; Picone, C.; Casteletti, L. On the wear and corrosion of plasma nitrided AISI H13. *Surf. Coat. Technol.* **2020**, *381*, 125216. [[CrossRef](#)]
44. Béjar, M.; Schnake, W.; Saavedra, W.; Vildósola, J. Surface hardening of metallic alloys by electrospark deposition followed by plasma nitriding. *J. Mater. Process. Technol.* **2006**, *176*, 210–213. [[CrossRef](#)]
45. Podgornik, B.; Vižintin, J.; Wänstrand, O.; Larsson, M.; Hogmark, S. Wear and friction behaviour of duplex-treated AISI 4140 steel. *Surf. Coat. Technol.* **1999**, *120*, 502–508. [[CrossRef](#)]

46. Podgornik, B.; Leskovšek, V.; Steiner-Petrovic, D.; Jerina, J. Load-carrying capacity of coated high-speed steel at room and elevated temperatures. In Proceedings of the 2nd Workshop on High Temperature Tribology-Mechanisms and Control of Friction & Wear, Luleå, Sweden, 18 March 2013; pp. 23–24.
47. Podgornik, B.; Hogmark, S.; Sandberg, O. Proper coating selection for improved galling performance of forming tool steel. *Wear* **2006**, *261*, 15–21. [[CrossRef](#)]
48. Podgornik, B.; Hogmark, S. Surface modification to improve friction and galling properties of forming tools. *J. Mater. Process. Technol.* **2006**, *174*, 334–341. [[CrossRef](#)]



© 2020 by the authors. Licensee MDPI, Basel, Switzerland. This article is an open access article distributed under the terms and conditions of the Creative Commons Attribution (CC BY) license (<http://creativecommons.org/licenses/by/4.0/>).